The effect of ligand efficacy on the formation and stability of a GPCR-G protein complex

Xiao Jie Yao[a], Gisselle Vélez Ruiz[b], Matthew R. Whorton[b], Søren G. F. Rasmussen[a], Brian T. DeVree[b], Xavier Deupi[c], Roger K. Sunahara[b,1], and Brian Kobilka[a,1]

[a]Department of Molecular and Cellular Physiology, Stanford University Medical School Department of Chemistry, Stanford University, Stanford, CA 94305; [b]Department of Pharmacology, University of Michigan Medical School, 1301 Medical Sciences Research Building III, Ann Arbor, MI 48109; and [c]Laboratori de Medicina Computacional, Unitat de Bioestadística, Facultat de Medicina, Universitat Autònoma de Barcelona, 08193 Bellaterra, Catalunya, Spain

Edited by Robert J. Lefkowitz, Duke University Medical Center, Durham, NC, and approved April 14, 2009 (received for review November 11, 2008)

G protein-coupled receptors (GPCRs) mediate the majority of physiologic responses to hormones and neurotransmitters. However, many GPCRs exhibit varying degrees of agonist-independent G protein activation. This phenomenon is referred to as basal or constitutive activity. For many of these GPCRs, drugs classified as inverse agonists can suppress basal activity. There is a growing body of evidence that basal activity is physiologically relevant, and the ability of a drug to inhibit basal activity may influence its therapeutic properties. However, the molecular mechanism for basal activation and inhibition of basal activity by inverse agonists is poorly understood and difficult to study, because the basally active state is short-lived and represents a minor fraction of receptor conformations. Here, we investigate basal activation of the G protein Gs by the β_2 adrenergic receptor (β_2AR) by using purified receptor reconstituted into recombinant HDL particles with a stoichiometric excess of Gs. The β_2AR is site-specifically labeled with a small, environmentally sensitive fluorophore enabling direct monitoring of agonist- and Gs-induced conformational changes. In the absence of an agonist, the β_2AR and Gs can be trapped in a complex by enzymatic depletion of guanine nucleotides. Formation of the complex is enhanced by the agonist isoproterenol, and it rapidly dissociates on exposure to concentrations of GTP and GDP found in the cytoplasm. The inverse agonist ICI prevents formation of the β_2AR-Gs complex, but has little effect on preformed complexes. These results provide insights into G protein-induced conformational changes in the β_2AR and the structural basis for ligand efficacy.

adrenergic | constitutive activity | receptor | conformation | inverse agonist

G protein-independent signaling pathways have been identified for a number of G protein-coupled receptors (GPCRs) (1–3); however, GPCR–G protein interactions represent the fundamental signaling interface, underlying the physiologic response to the majority of hormones and many neurotransmitters. Crystal structures of G proteins have been obtained in both active and inactive states (4–6), and structures of bovine rhodopsin (7–12), squid rhodopsin (13, 14), bovine opsin (15, 16), the human β_2AR (17–19), the turkey β_1AR (20), and the adenosine A2a receptor (21) have been reported. However, relatively little is known about the active-state GPCR-G protein complex.

The active-state GPCR-G protein complex will be defined as the physical association between a GPCR and a G protein that promotes GTP binding to the Gα subunit. This complex can be identified by the specific allosteric effects that each protein imposes on the other. Agonist-bound GPCRs promote exchange of GDP for GTP on the Gα subunit. G protein effects on receptor structure are more difficult to detect, but agonist binding affinity for many GPCRs is enhanced when complexed with a G protein. This effect was originally demonstrated for the β_2AR (22) and led to the ternary complex model of receptor activation (23). The enhanced agonist affinity observed for the active-state complex is abolished by both GTP and GDP suggesting that the bound G protein is nucleotide-free (24).

The active-state complex should be distinguished from other types of physical association or co-localization of GPCRs and G proteins that may be observed in cells and may be important for signal transduction. Recently it has been possible to study GPCR–G protein interactions in cells by using FRET between components tagged with fluorescent and/or luminescent proteins (25–27). These studies provide evidence that a fraction of receptors and G proteins may exist in a precoupled or preassociated state. These associations may occur through direct receptor–G protein interactions, or through interactions with common scaffolding proteins. However, this precoupled or preassociated state probably differs from the active-state or ternary complex as defined above, because G protein-dependent high-affinity agonist binding is not observed at GTP and GDP concentrations present in intact cells (28, 29). Thus, in the presence of cytosolic guanine nucleotides, the active-state complex would be short-lived.

For many GPCRs, the active-state complex can form in the absence of agonists leading to a certain level of basal, agonist-independent activity also called constitutive activity. There is a growing appreciation that drugs that inhibit basal activity, called inverse agonists, may be more effective therapeutics for some indications than neutral antagonists—drugs that competitively inhibit agonist binding but have little or no effect on basal activity (30).

Little is known about the mechanism for basal activity and inverse agonism. Here, we use site-specific labeling of β_2AR with a conformationally sensitive fluorescent probe together with recombinant HDL particles (31), a highly efficient reconstitution system, to investigate the active-state complex. This experimental system allows us to directly monitor ligand- and G protein-induced conformational changes in the β_2AR. We observe that monomeric β_2AR forms a stable complex with the Gs heterotrimer in the absence of guanine nucleotides. This complex can be detected by changes in the fluorescence of labeled β_2AR. Conformational changes induced in the β_2AR by Gs alone or by agonist alone result in similar changes in the fluorescence of labeled β_2AR. The β_2AR-Gs complex rapidly dissociates in the presence of both GDP and GTP. A saturating concentration of the inverse agonist ICI-118,551 does not disrupt the preformed complex, but prevents complex formation. In contrast, the neutral antagonist alprenolol has little effect on the stability of the complex nor does it prevent complex formation. These results provide insights into G protein-induced changes in β_2AR

Author contributions: X.D., R.K.S., and B.K. designed research; X.J.Y., G.V.R., M.R.W., S.G.F.R., and B.T.D. performed research; X.J.Y., X.D., R.K.S., and B.K. analyzed data; and R.K.S. and B.K. wrote the paper.

The authors declare no conflict of interest.

This article is a PNAS Direct Submission.

Freely available online through the PNAS open access option.

[1]To whom correspondence may be addressed. Email: kobilka@stanford.edu or sunahara@umich.edu.

This article contains supporting information online at www.pnas.org/cgi/content/full/0811437106/DCSupplemental.

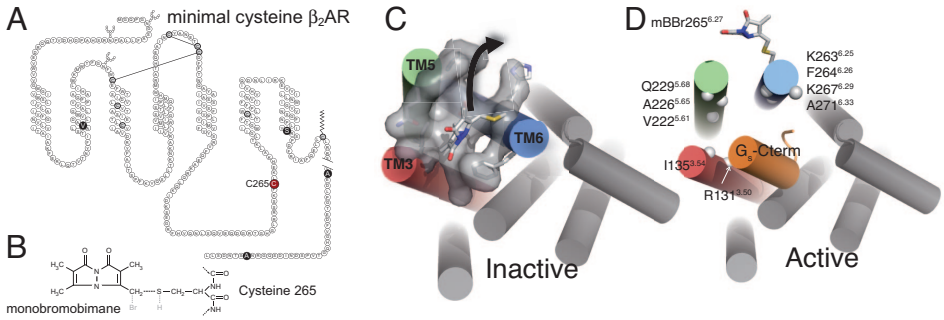

Fig. 1. Site-specific labeling of purified β_2AR with monobromobimane. (*A*) Sequence and secondary structure of the human β_2AR showing sites where reactive cysteines were mutated to the indicated amino acid (black circles with white letters). C265 is shown in red. The remaining cysteines (gray circles) are not reactive toward monobromobimane. (*B*) The structure of bimane covalently bound to C265 after reaction with monobromobimane. (*C*) In the inactive structure of the β_2AR, bimane bound to C265 is predicted to occupy a cavity between TM3, TM5, and TM6. When TM6 adopts an active conformation (because of agonist binding or due to constitutive activity), bimane is displaced (black arrow) out of this cavity to a more polar environment, which is detected as a change in fluorescence intensity and λ_{MAX}. (*D*) A model of the active state of the β_2AR in complex with the carboxyl terminal peptide of $G\alpha_s$, based on the crystal structure of opsin in complex with a transducin peptide. The amino acids at the positions marked by solid spheres are predicted to form interactions with $G\alpha_s$. The residues of the β_2AR are numbered according to their position in the sequence followed by the Ballesteros general number (49) in superscript. In this numbering scheme, the most conserved residue within each helix is designated x.50, where x is the number of the transmembrane helix. All other residues on that helix are numbered relative to this conserved position. The model of the active conformation of β_2AR shown in Fig. 1*D* was built by homology modeling using the β_2AR (2RH1) and opsin (3CAP) structures as templates. The $G\alpha_s$ fragment bound to the active-like β_2AR was modeled by threading the 11 C-terminal residues of $G\alpha_s$ on the structure of the synthetic peptide derived from the carboxy terminus of $G\alpha_t$ bound to opsin. The surface of the cytoplasmic side of the receptor shown in Fig. 1*C* was calculated with CastP (50). Homology models and figures were prepared with PyMOL (DeLano WL (2002) *The PyMOL Molecular Graphics System*. Available at http://www.pymol.org).

structure and the effect of ligand efficacy on the formation and stability of the β_2AR-Gs complex.

Results and Discussion

Site-Specific Labeling of β_2AR with Monobromobimane, an Environmentally Sensitive Fluorophore. To detect agonist and G protein-induced conformational changes in the β_2AR, we introduced a conformationally sensitive fluorophore adjacent to the G protein-coupling region of transmembrane segment (TM) 6. We previously showed that fluorophores covalently bound to C265 at the cytoplasmic end of TM6 (Fig. 1) are capable of detecting agonist-induced conformational changes (32–34). C265 is well positioned to detect conformational changes associated with G protein activation. The recent crystal structure of the human β_2AR (17) predicts that monobromobimane bound to C265 lies in a relatively nonpolar pocket formed at the interface between TMs 3, 5 and 6 (Fig. 1*C*). The recent structure of opsin bound to the carboxyl terminus of the Gα-subunit of transducin (16) shows that the G protein interacts with residues in the inner side of the cytoplasmic TM5 and TM6. A similar pattern of interaction between the β_2AR and Gs would involve residues V222$^{5.61}$, A226$^{5.65}$, and Q229$^{5.68}$ in TM5, and K263$^{6.25}$, F264$^{6.26}$, K267$^{6.29}$, and A271$^{6.33}$ in TM6, in the vicinity of C265$^{6.27}$ (see Fig. 1*D*). Conformational changes associated with activation of the β_2AR would be expected to displace bimane bound to C265 to a more polar environment.

C265 is highly reactive to labeling with polar, cysteine-reactive fluorophores (19, 32, 35). The remaining reactive cysteines can be removed by mutagenesis (C77V, C327S, C378A, and C406A) without altering receptor function (35) (Fig. 1*A*). We previously found that the receptor palmitoylation site (C341) is not reactive (32). Stable palmitoylation of C341 was confirmed in the crystal structure of the β_2AR where protein was purified and alkylated with 4 mM iodoacetamide (100-fold molar excess) under the same conditions. Both the palmitate bound to C341 and iodoacetamide bound to C265 were clearly ordered in the crystal structure.

The modified receptor was expressed in Sf9 insect cells by using recombinant baculovirus technology and purified as previously described (35). Purified β_2AR was labeled with an equivalent amount of monobromobimane. This modified β_2AR labeled at Cys-265 with monobromobimane will be referred to as mB-β_2AR. Monobromobimane is an ideal fluorophore for these experiments because its small size (approximately equivalent to tryptophan, Fig. 1*B*) and short linker, together with its high sensitivity to the polarity of its molecular environment. These properties make it highly sensitive for detecting conformational changes without interfering with receptor function. Any ligand or G protein-induced movement at the cytoplasmic end of TMs 3, 5, or 6 would be expected to change the molecular environment, and therefore the fluorescence properties, of bimane bound to C265.

Agonist- and Gs-Induced Changes in mB-β_2AR Reconstituted into Recombinant HDL Particles. β_2AR requires a lipid bilayer to efficiently couple to Gs. Whorton et al. recently showed that purified β_2AR can be reconstituted into recombinant HDL particles (rHDL) as monomers, and that monomeric β_2AR couples efficiently to Gs (31). Thus, mB-β_2AR was reconstituted into rHDL, and the response to the agonist isoproterenol (ISO) was determined. Fig. 2*A* shows the emission spectra of mB-β_2AR in the absence of G protein but in the presence of increasing concentrations of the full agonist ISO. We observe a dose-dependent decrease in fluorescence intensity and an increase in the maximal emission wavelength (λ_{MAX}) of 15 nm (Fig. 2*A*). The concentration-dependent effects of ISO on intensity and λ_{MAX} are shown in supporting information (SI) Fig. S1 *A* and *B*. It should be noted that the EC_{50} for the fluorescence dose–response curve (Fig. S1*A*, blue curve) is approximately 3-fold higher than the IC_{50} for ISO in a conventional competition binding experiment (Fig. 2*D*, black curve). This difference may in part be due to the fact that conformational assays were performed at much higher receptor concentrations (50–100 nM) than were used for conventional ligand binding experiments. Consequently, responses to lower concentrations of ligand may be influenced by ligand depletion. It is also possible that an agonist binding event is not always associated with a conformational change. Agonists such as ISO have relatively low affinity and very rapid on and off rates. ISO can occupy the binding pocket for long enough time to compete with a radiolabeled

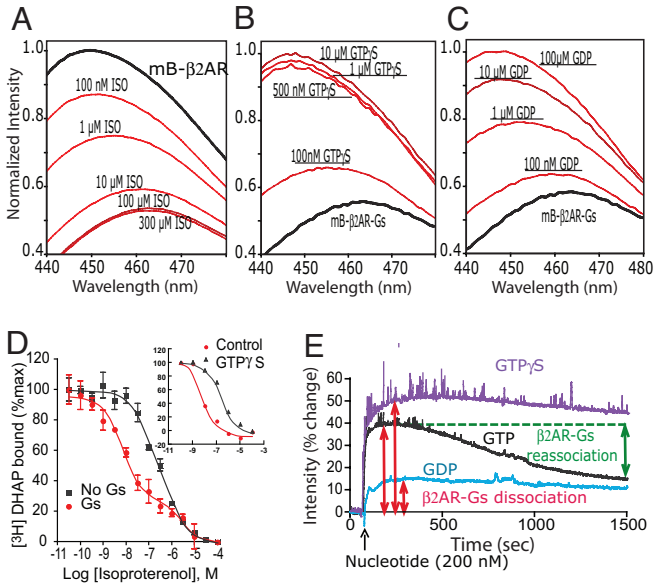

Fig. 2. Reconstitution of purified bimane-labeled β_2AR (mB-β_2AR) and Gs into rHDL particles. (*A*) Bimane emission spectra of reconstituted mB-β_2AR in the absence (black spectrum) and presence of increasing concentrations of the agonist ISO (red spectra). Agonist-induced conformational changes lead to a decrease in fluorescence intensity of bimane and a shift in the λ_{MAX}. (*B* and *C*) Bimane emission spectra of mB-β_2AR reconstituted with Gs in the absence of agonist or nucleotides (black spectrum) and in the presence of increasing concentrations of GTPγS (*B*) and GDP (*C*) (red spectra). All spectra were normalized to the unliganded, uncoupled state of mB-β_2AR. For experiments in *A*, this state was the value for the sample without ligand. For experiments in *B* and *C*, this state was the value obtained following the addition of 10 μM GTPγS. Each spectrum in *A*–*C* represents the average of 3 independent experiments. (*D*) ISO inhibition of [^{3}H]DHAP binding to mB-β_2AR in rHDL in the presence (red) and absence (black) of Gs. *Inset* shows the effect of 10 μM GTPγS on ISO bind affinity to mB-β_2AR reconstituted with Gs. These data were fit by using Prism 5.0 (Graphpad). (*E*) Time-scan of fluorescence monitored at 450 nm. The effect of 200 nM GTP, GTPγS, and GDP on mB-β_2AR-Gs are compared. GTP induces dissociation of mB-β_2AR and Gs followed by reformation of the complex after GTP hydrolysis.

antagonist, but this binding event may not always be associated with an activating conformational change.

Purified Gs heterotrimer ($G\alpha_S\beta_1\gamma_2$) was added to rHDL containing mB-β_2AR at a ratio of 10 Gs per β_2AR monomer to ensure that mB-β_2AR would have access to at least 1 Gs trimer [during the reconstitution, some Gs is lost because of aggregation due to removal of detergent (31)]. Gs induces a high affinity state for the agonist ISO (K_i 1.6 nM in the presence of Gs compared with 840 nM in the presence of Gs and GTPγS, or mB-β_2AR alone, Fig. 2*D*) comparable to what is observed in unlabeled β_2AR (31). Thus, modification of C265 with bimane does not interfere with G protein coupling. Using these reconstitution conditions, we observed that more than 80% of mB-β_2AR is in the G protein-dependent high-affinity agonist binding state.

Fig. 2 *B* and *C* show the emission spectra of mB-β_2AR after reconstitution with Gs. The λ_{MAX} of mB-β_2AR-Gs fluorescence is similar to that observed for mB-β_2AR following the addition of isoproterenol (Fig. 2*A*). The effect of Gs on mB-β_2AR fluorescence can be revealed by uncoupling the receptor from Gs by using either GTPγS or GDP. The addition of GTPγS or GDP results in an increase in fluorescence intensity and a 15 nm decrease in the λ_{MAX} (Figs. 2 *B* and *C* and S1 *C* and *D*) to a value similar to that observed in unliganded mB-β_2AR before reconstitution (Fig. 2*A*). GTPγS is more potent at uncoupling mB-β_2AR from Gs compared with GDP, consistent with previous studies indicating that Gs coupled to the β_2AR has a higher affinity for GTPγS than for GDP (24). The concentration-dependent effects of GTPγS and GDP on intensity and λ_{MAX} of mB-β_2AR are shown in Fig. S1 *C* and *D*. The effect of GDP on mB-β_2AR-Gs fluorescence may be unexpected given the prevailing view that the receptor binds preferentially to Gs-GDP and induces GDP release. If mB-β_2AR and Gs-GDP form a complex, this complex does not exhibit the properties of the active state complex as defined above, because cytosolic concentrations of GDP can disrupt Gs dependent high-affinity agonist binding (24). An alternate explanation for these observations is that the β_2AR binds to and stabilizes a small fraction of nucleotide-free Gs that is in equilibrium with Gs-GDP.

Fig. 2*E* shows a time course of the effect of 200 nM GTP, GTPγS, and GDP on mB-β_2AR fluorescence intensity measured at 450 nm. As expected, all guanine nucleotides induce a rapid increase in fluorescence consistent with the disruption of the active-state mB-β_2AR-Gs complex. The effect at this concentration is larger for GTP and GTPγS compared with GDP. After the initial increase in fluorescence, we observe a decrease in fluorescence for GTP, but not for GDP or GTPγS. This decrease can be explained by the ability of Gs to hydrolyze GTP, but not GDP or GTPγS. Thus, on the initial dissociation of the mB-β_2AR-Gs complex, GTP is hydrolyzed to GDP and some of the mG-β_2AR can reassociate with Gs.

These fluorescence studies show that mB-β_2AR and Gs form an active-state complex (as defined in the introductory paragraphs) in the absence of an agonist. The agonist ISO and Gs induce similar changes in the fluorescence intensity and λ_{MAX} of mB-β_2AR. These changes are consistent with movement of the fluorophore to a more polar environment that could be achieved by a clockwise rotation and/or outward movement of TM6 relative to TM3 and TM5 (Fig. 1*D*). This movement is in agreement with the changes observed in rhodopsin by double electron–electron resonance (DEER) spectroscopy (36), as well as conformational differences between rhodopsin and opsin (15), and previous biophysical and mutagenesis studies on the β_2AR (37–39). The fact that both Gs and the agonist ISO induce similar changes in fluorescence is compatible with the hypothesis that they independently induce similar changes in receptor structure and is consistent with the allosteric effect of Gs on agonist affinity and of agonists on Gs activation. Nevertheless, we cannot exclude the possibility that similar changes in mB-β_2AR fluorescence could result from different conformational changes in the β_2AR.

The Effect of Ligand Efficacy on mB-β_2AR-Gs Coupling. The efficiency with which mB-β_2AR couples to Gs in rHDL particles in the absence of agonist reflects the receptor's intrinsic basal activity. The high effective concentration of Gs and the capacity to trap mB-β_2AR in this active Gs-coupled state in the absence of guanine nucleotides has allowed us to visualize this complex. In cells, however, GDP concentrations exceed 10 μM (28, 29), levels that would destabilize this complex as shown by the capacity of GDP to reverse the effects of Gs on mB-β_2AR (Fig. 2*B*). Nevertheless, our ability to trap this complex and monitor it through a conformationally sensitive fluorescent reporter allows us to examine the effects of ligand efficacy on the formation and stability of this otherwise transient complex. For the purpose of our discussion, we will assume that a decrease in intensity and increase in λ_{MAX} of mB-β_2AR-Gs is a reflection of the stability of the active-state complex. This assumption is based on the observation that conditions known to disrupt interactions between β_2AR and Gs such as GTPγS and detergents result in an increase in intensity and a decrease in λ_{MAX} (Fig. 2*B*). However, we acknowledge that changes in λ_{MAX} and intensity may not reflect a proportional change in the affinity of β_2AR for Gs; moreover, it is possible that β_2AR and Gs remain associated in a manner that is not detected by bimane on C265.

Agonist. In Fig. 3 we compare the effects of an agonist, a neutral antagonist, and an inverse agonist on mB-β_2AR-Gs. Because

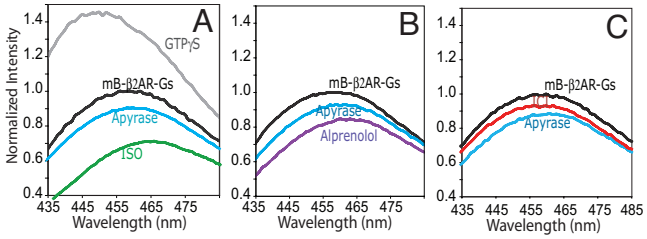

Fig. 3. The effect of ligands having different efficacies on the stability of mB-β_2AR-Gs. Emission scans were performed on mB-β_2AR-Gs complex obtained from a single reconstitution. For each treatment (apyrase, ISO, alprenolol, ICI, or GTPγS), a baseline scan was performed on mB-β_2AR-Gs alone (black spectrum), and subsequent scans were normalized to this baseline scan. (*A*) The gray spectrum was taken 10 min after the addition of 10 μM GTPγS to mB-β_2AR-Gs. This treatment uncouples Gs from mB-β_2AR. The blue spectrum shows the effect of a 40-min incubation of mB-β_2AR-Gs with apyrase to remove residual GDP. (*A–C*) The effect of ligands was determined after 40-min pretreatment with apyrase (blue) followed by a 60-min incubation with the ligand. *A*: ISO, green; *B*: alprenolol, purple; *C*: ICI, red. This experiment is representative of 3 independent experiments.

there is slight variability in receptor to G protein stoichiometry between reconstitutions, these comparisons were performed on the same preparation. Fig. 3*A* shows the baseline spectrum of the mB-β_2AR-Gs complex before (black) and after (gray) the addition of 10 μM GTPγS, which completely dissociates the complex. The reconstitutions are typically contaminated with a low concentration of GDP needed to stabilize purified Gs. This residual GDP can be removed by the addition of apyrase, a nonselective nucleotide pyrophosphatase. As shown in Fig. 3*A*, a 40-min treatment with apyrase reverses the uncoupling effect of residual GDP resulting in a small decrease in the intensity of mB-β_2AR (blue spectrum). The addition of the agonist ISO after apyrase treatment causes a further decrease in intensity and a rightward shift in λ_{MAX} (Fig. 3*A*, green spectrum). The fact that ISO induces a change in fluorescence intensity on top of that induced by Gs and apyrase suggests that a higher fraction of mB-β_2AR couples to Gs in the presence of agonist and/or the conformation of the β_2AR in the presence of agonist and Gs is different from that in the presence of Gs alone. The maximal effect of ISO on mB-β_2AR-Gs fluorescence occurs at a lower agonist concentration than observed in the absence of Gs (Fig. S2) and is consistent with the effect of Gs on ISO binding affinity (Fig. 2*D*).

Neutral antagonist. By definition, neutral antagonists inhibit binding of agonists, partial agonists, and inverse agonists at the orthosteric binding site of GPCRs, but do not alter their basal receptor activity. It has been difficult to identify true neutral antagonists for the β_2AR, as most compounds display some partial agonist or inverse agonist activity when applied in sensitive signaling assays (40, 41). Nevertheless, alprenolol comes very close to exhibiting the properties of a neutral antagonist, having only very weak partial agonist activity or weak inverse agonist activity, depending on the assay (40, 41). Alprenolol has no significant effect on the fluorescence of mB-β_2AR alone (see below). The effect of alprenolol on mB-β_2AR-Gs was examined following the removal of residual GDP with apyrase. As shown in Fig. 3B, alprenolol (purple spectrum) induces a small decrease in the intensity and red shift in the λ_{MAX} of mB-β_2AR-Gs that has been treated with apyrase. Thus, alprenolol does not induce dissociation of the mB-β_2AR-Gs complex, and may enhance mB-β_2AR-Gs coupling to a small extent, perhaps related to a low partial agonist activity (41).

Inverse agonist. In contrast to neutral antagonists, inverse agonists inhibit basal, agonist-independent activation of G proteins. Although the precise mechanism for the action of inverse agonists is not completely understood, they may prevent receptor-G protein complex formation, destabilize preformed complexes, or both. Here, we studied the effect of ICI-118,551 (ICI), one of the most efficacious inverse agonists for the β_2AR (41), on mB-β_2AR-Gs fluorescence (Fig. 3*C*, red spectrum). mB-β_2AR-Gs was first treated with apyrase to remove residual GDP. Following a 60-min incubation at room temperature, ICI induced only a small reversal of fluorescence change induced by Gs and apyrase (compare blue and red spectra). These data show that ICI is much less effective at disrupting preformed receptor-G protein complexes than is GTPγS (Fig. 3*A*).

The effect of ligands on β_2AR-Gs complex formation. The relatively subtle effect of ICI on the stability of the receptor-G protein complex does not explain the inhibitory effect of ICI observed in signaling assays. An alternative mechanism for ICI efficacy, is that the ICI-bound β_2AR does not couple efficiently to Gs. To monitor the effect of ICI on the association of β_2AR and Gs we incubated mB-β_2AR reconstituted in rHDL in the presence or absence of ligands. We then added purified Gs and monitored changes in fluorescence. It should be noted that the amount of Gs that can be added is limited by the detergent in the Gs preparation, consequently the Gs-induced changes in mB-β_2AR are not as large as those observed in Figs. 2 and 3, where the reconstitution was done in the presence of a detergent binding resin. In the absence of ligand, Gs coupling to the β_2AR results in an 18% decrease in intensity and a 5-nm red shift in λ_{MAX} (Fig. 4*A*). The addition of 1 μM ISO to mB-β_2AR resulted in a 25% decrease in intensity and a 7-nm red shift in λ_{MAX}. The addition of Gs resulted in a further decrease in both intensity and λ_{MAX} (Fig. 4*B*). In contrast, no change in fluorescence was observed following the addition of Gs to mB-β_2AR that had been incubated for 15 min with 1 μM ICI (Fig. 4*C*). Like ICI, the neutral antagonist alprenolol had no effect on mB-β_2AR fluorescence. However, in contrast to ICI, alprenolol did not prevent Gs-induced changes in mB-β_2AR intensity and λ_{MAX} (Fig. 4*D*). In

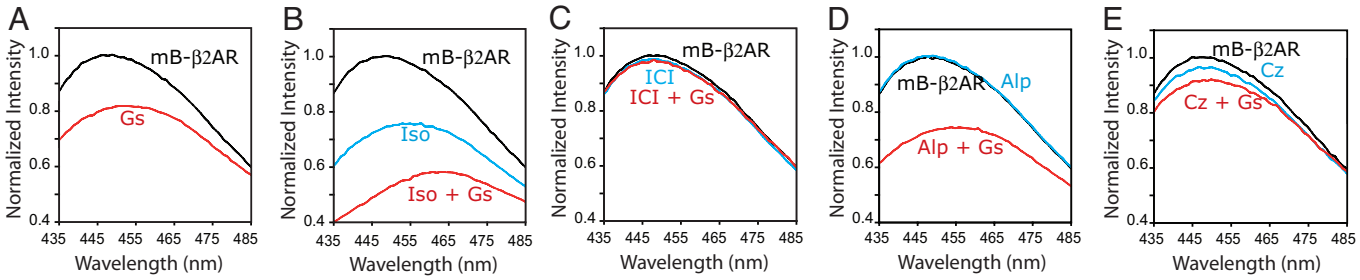

Fig. 4. The effect of ligand efficacy on Gs-induced changes in mB-β_2AR fluorescence. Initial emission scans (black spectra) of mB-β_2AR were obtained, then scans were repeated after a 15-min incubation with the indicated ligands (blue spectra). A concentrated solution of Gs was added (1:100 dilution of an 8 mg/mL solution), and emission scans were repeated after 8 min (red spectra). Preliminary studies showed that the effect of Gs was complete at 6 min. Ligands: *A*, no ligand; *B*, isoproterenol (Iso); *C*, ICI; *D*, alprenolol (Alp); *E*, carazolol (Cz). These scans are representative of 3 independent experiments.

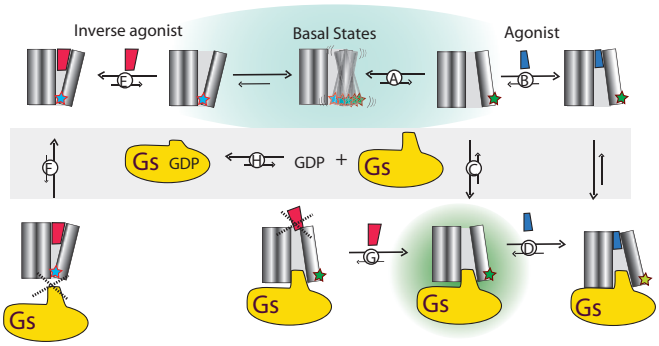

Fig. 5. Conceptual model depicting the dynamic behavior of β_2ARs. In the absence of a ligand, the β_2AR exists in an ensemble of basal states in dynamic equilibrium (blue background). Agonists and inverse agonists bind to and stabilize distinct substates. The nucleotide free form of the G protein Gs can also bind to and stabilize an active state of the β_2AR (green background). The different equilibrium processes between the receptor and its ligands and the receptor and the G protein Gs are displayed (*A–H*) and are described in detail in the text. Note that for each of these equilibria, the relative size of the arrows indicates the displacement of the reaction.

fact, these changes were larger than those observed for unliganded mB-β_2AR, suggesting alprenolol has partial agonist activity. We also examined carazolol, the partial inverse agonist used to obtain the crystal structures of the β_2AR. We observed a small (approximately 3%) decrease in intensity, but no change in λ_{MAX} following incubation with 1 μM carazolol (Fig. 4*E*). Gs induced a further 5% decrease in intensity and a 2-nm shift in λ_{MAX}. In comparison to unliganded receptor (Fig. 4*A*), carazolol appeared to partially inhibit Gs-induced changes; however, it was not as effective as ICI. These results show that the inverse agonist ICI is most efficacious in preventing Gs-induced changes in mB-β_2AR, underlying its effectiveness as an inverse agonist in signaling assays.

It should be noted that the lack of changes in mB-β_2AR fluorescence on binding to ICI does not necessarily mean that ICI does not induce or stabilize a conformation distinct from unliganded receptor. It only suggests that conformational changes occurring on ICI binding may not result in a change in the environment around bimane on C265. Previous studies using different fluorescent approaches observed conformational changes on binding ICI to the β_2AR (42) and yohimbine for the α_{2A} adrenergic receptor (43). The fact that ICI prevents Gs-induced conformational changes observed in the absence of ligand is consistent with a distinct conformation.

Structural Insights into the Active State Complex, Basal Activity, and Ligand Efficacy. The mechanism by which Gs couples to agonist-free receptor is not known. However, the recent structure of a complex between opsin and the carboxyl-terminal peptide of transducin, suggests that substantial conformational changes are needed in the inactive structure of the β_2AR to permit a similar docking of the carboxyl terminus of Gα_S (Fig. 1 *C* and *D*). Evidence from fluorescence lifetime studies on purified β_2AR shows that the unliganded receptor is structurally dynamic (44) and exists in an ensemble of basal conformational states (Fig. 5). Although an active state represents a minor fraction of this ensemble (Fig. 5*A*), this state would be stabilized by binding to either the agonist ISO (Fig. 5*B*) or the G protein Gs (Fig. 5*C*).

As shown in Fig. 3*A*, the agonist ISO (green spectrum) induces a further decrease in the fluorescence intensity and increase in the λ_{MAX} of the mB-β_2AR-Gs complex. This result could be because of a change in the equilibrium favoring the formation of the complex (Fig. 5*D*), or to a further change in the structure of the mB-β_2AR-Gs complex. We cannot distinguish between these two possibilities; nevertheless; these observations have implications for efforts to obtain a high-resolution structure of the active state of the β_2AR and possibly other GPCRs. Saturating concentrations of an agonist alone (Fig. 5*B*) cannot induce the same change in intensity and λ_{MAX} as that stabilized by both Gs and ISO (Fig. 5*D*). The results are in agreement with earlier fluorescence lifetime studies on the β_2AR showing that the agonist ISO does not stabilize a single active conformation (44).

Analogous to agonists, the inverse agonist ICI binds to and stabilizes a minor fraction of the ensemble of basal conformational states, in this case corresponding to an inactive conformation (Fig. 5*E*). The capacity of ICI to prevent formation of the mB-β_2AR-Gs complex (Fig. 4*C*) suggests that the conformation stabilized by the inverse agonist cannot couple to Gs (Fig. 5*F*). Similarly, the fact that 1 μM ICI (100-fold greater than the K_d) has little effect on the preformed mB-β_2AR-Gs complex (Fig. 3*C*) suggests that it cannot bind to Gs-coupled β_2AR (Fig. 5*G*). This result is in agreement with predictions of the extended ternary complex model (45, 46) and previous studies showing that binding sites for [^{3}H]-ICI-118,551 were reduced in cells expressing high levels of Gs (47). These effects can also be rationalized in light of the crystal structure of the inactive, inverse agonist-bound β_2AR. ISO is 40% smaller in volume than the inverse agonist carazolol present in the β_2AR crystal structure. Thus, the binding site of the ISO-bound receptor will have to readjust to satisfy all of the binding interactions predicted for the agonist ISO (18).

Relevance to Cellular Signal Transduction. We were able to characterize the properties of the mB-β_2AR-Gs complex by reconstituting purified β_2AR and Gs under conditions that would not be found in a living cell. Reconstitutions were performed at low GDP concentrations, and GDP was further reduced by using apyrase. In the presence of apyrase, virtually all Gs will be in the nucleotide-free state (Fig. 5*H*). Thus, it is possible to trap both unliganded and agonist-bound mB-β_2AR-Gs complexes. Under these conditions, the inverse agonist is unable to disrupt the complex (Fig. 5*G*), most likely because of allosteric effects of the G protein on the ligand binding pocket. However, in the context of a cell, where concentrations of GDP may exceed 10 μM, the formation of an active state β_2AR-Gs complex will be a relatively rare event governed by 2 equilibria: 1 for the conformational transition to an active state of the receptor (Fig. 5*A*), and 1 for the formation of nucleotide free Gs (Fig. 5*H*). Once the nucleotide-free β_2AR-Gs complex is formed, it would be rapidly disrupted on binding of either GDP or GTP. Thus, although ICI may not be able to disrupt the β_2AR-Gs complex, these complexes are relatively rare and short-lived. ICI efficacy is due primarily to binding to the receptor and stabilizing a conformation that is unable to couple to Gs (Fig. 5*E*). In contrast, agonists facilitate the formation of the complex by increasing the fraction of β_2AR in an active conformation (Fig. 5*B*), and possibly by stabilizing a conformation in the β_2AR that allosterically reduces the affinity of Gs for GDP.

In conclusion, our studies examine the allosteric interaction between ligand binding and Gs coupling by using a conformational reporter on the β_2AR, and they provide a structural framework for understanding the concept of basal activity and ligand efficacy. Agonists and Gs induce similar changes in the fluorescence intensity and the λ_{MAX} of mB-β_2AR-Gs, suggesting they may induce a similar conformational change involving TM6. The complex formed between the β_2AR and Gs in the absence of agonist is stable in the absence of guanine nucleotides. A neutral antagonist has little effect on the formation of the β_2AR Gs complex, whereas an inverse agonist prevents complex formation. Neither antagonist nor inverse agonist promotes dissociation, whereas both GDP and GTP rapidly reverse Gs-induced changes in mB-β_2AR fluorescence. These findings

provide insights into the structural basis of drug efficacy, that is, how different chemical structures are ultimately translated into divergent behaviors through the modulation of the interaction between the receptor and the G protein.

Materials and Methods

Expression, Purification, and Labeling of β_2AR. Construction and characterization of a modified β_2AR where 4 reactive cysteines were mutated (C77V, C327S, C378A, and C406A) was previously described (35). The modified β_2AR was expressed in Sf9 insect cells by using recombinant baculovirus and purified by sequential M1 antibody affinity and alprenolol affinity chromatography as previously described (35). Purified receptor and monobromobimane were mixed at same molarity and incubated overnight on ice in the dark. The fluorophore-labeled receptor was purified right before use by gel filtration.

In Vitro Reconstitution of β_2AR and Gs into rHDL. Wild-type human apoA-I was purified from human serum as described in detail in Whorton et al. (31). Gs heterotrimer ($G\alpha s_s$, his6-β_1, γ_2) was expressed in Sf9 cells and purified essentially as previously described (48). Monobromobimane labeled β_2AR was reconstituted into rHDL particles together with purified Gs heterotrimer as previously described (31). Competition radioligand binding experiments were performed as previously described (31).

Fluorescence Spectroscopy. Fluorescence spectroscopy experiments were performed on a Spex FluoroMax-3 spectrofluorometer (Jobin Yvon Inc.) with photon counting mode by using an excitation and emission bandpass of 4 nm. For each scan, the final concentration of receptor range from 50–100 nM. For emission scans, excitation was set at 370 nm and emission was measured from 435–485 nm with an integration time of 0.5 s/nm. To determine the effect of ligands, the spectra were taken after 15 min incubation with the drugs. For time course experiments, excitation was at 370 nm, and emission was monitored at 450 nm. All experiments were performed at 25 °C, and the sample underwent constant stirring. Fluorescence intensity was corrected for dilution by ligands in all experiments and normalized to the initial value. Fluorescence intensity was corrected for background fluorescence from buffer and ligands in all experiments. All of the compounds tested had an absorbance of <0.01 at wavelengths between 370 nm and 485 nm at the concentrations used, excluding any inner filter effect in the fluorescence experiments.

ACKNOWLEDGMENTS. The authors would like to thank Richard Neubig (University of Michigan) and Leonardo Pardo (Universitat Autonoma de Barcelona) for critical discussion. This work was supported by the Lundbeck Foundation (S.G.F.R.); Ministerio de Ciencia e Innovación, Government of Spain, through the Ramón y Cajal program (X.D.); National Institute of Neural Disorders and Stroke Grant RO1-NS28471 (to B.K.); the Mather Charitable Foundation (B.K.); National Institute of General Medical Sciences Grants RO1-GM083118 (to B.K. and R.K.S.) and RO1-GM068603 (to R.K.S.); Michigan Diabetes Research and Training Center Grant, National Institute of Diabetes and Digestive and Kidney Diseases, P60DK-20572 (to R.K.S.); and the University of Michigan Biological Sciences Scholars Program (R.K.S.).

1. Lefkowitz RJ, Shenoy SK (2005) Transduction of receptor signals by beta-arrestins. *Science* 308:512–517.
2. Luttrell LM, Lefkowitz RJ (2002) The role of beta-arrestins in the termination and transduction of G-protein-coupled receptor signals. *J Cell Sci* 115:455–465.
3. Azzi M, et al. (2003) Beta-arrestin-mediated activation of MAPK by inverse agonists reveals distinct active conformations for G protein-coupled receptors. *Proc Natl Acad Sci USA* 100:11406–11411.
4. Sunahara RK, Tesmer JJ, Gilman AG, Sprang SR (1997) Crystal structure of the adenylyl cyclase activator $G_{s\alpha}$. *Science* 278:1943–1947.
5. Sondek J, Lambright DG, Noel JP, Hamm HE, Sigler PB (1994) GTPase mechanism of G-proteins from the 1.7-Å crystal structure of transducin α-GDP AlF^-_4. *Nature* 372:276–279.
6. Kreutz B, et al. (2006) A new approach to producing functional G alpha subunits yields the activated and deactivated structures of G alpha(12/13) proteins. *Biochemistry* 45:167–174.
7. Palczewski K, et al. (2000) Crystal structure of rhodopsin: A G protein-coupled receptor. *Science* 289:739–745.
8. Okada T, et al. (2000) X-ray diffraction analysis of three-dimensional crystals of bovine rhodopsin obtained from mixed micelles. *J Struct Biol* 130:73–80.
9. Okada T, et al. (2002) Functional role of internal water molecules in rhodopsin revealed by X-ray crystallography. *Proc Natl Acad Sci USA* 99:5982–5987.
10. Teller DC, Okada T, Behnke CA, Palczewski K, Stenkamp RE (2001) Advances in determination of a high-resolution three-dimensional structure of rhodopsin, a model of G-protein-coupled receptors (GPCRs). *Biochemistry* 40:7761–7772.
11. Okada T, et al. (2004) The retinal conformation and its environment in rhodopsin in light of a new 2.2 Å crystal structure. *J Mol Biol* 342:571–583.
12. Li J, Edwards PC, Burghammer M, Villa C, Schertler GF (2004) Structure of bovine rhodopsin in a trigonal crystal form. *J Mol Biol* 343:1409–1438.
13. Murakami M, Kouyama T (2008) Crystal structure of squid rhodopsin. *Nature* 453:363–367.
14. Shimamura T, et al. (2008) Crystal structure of squid rhodopsin with intracellularly extended cytoplasmic region. *J Biol Chem* 283:17753–17756.
15. Park JH, Scheerer P, Hofmann KP, Choe HW, Ernst OP (2008) Crystal structure of the ligand-free G-protein-coupled receptor opsin. *Nature* 454:183–187.
16. Scheerer P, et al. (2008) Crystal structure of opsin in its G-protein-interacting conformation. *Nature* 455:497–502.
17. Rasmussen SGF, et al. (2007) Crystal structure of the human β_2 adrenergic G-protein-coupled receptor. *Nature* 450:383–387.
18. Rosenbaum DM, et al. (2007) GPCR engineering yields high-resolution structural insights into β_2-adrenergic receptor function. *Science* 318:1266–1273.
19. Cherezov V, et al. (2007) High-resolution crystal structure of an engineered human β_2-adrenergic G protein-coupled receptor. *Science* 318:1258–1265.
20. Warne T, et al. (2008) Structure of a β_1-adrenergic G-protein-coupled receptor. *Nature* 454:486–491.
21. Jaakola VP, et al. (2008) The 2.6 Angstrom crystal structure of a human A_{2A} adenosine receptor bound to an antagonist. *Science* 322:1211–1217.
22. Ross EM, Maguire ME, Sturgill TW, Biltonen RL, Gilman AG (1977) Relationship between the β-adrenergic receptor and adenylate cyclase. Studies of ligand binding and enzyme activity in purified membranes of S49 lymphoma cells. *J Biol Chem* 252:5761–5775.
23. De Lean A, Stadel JM, Lefkowitz RJ (1980) A ternary complex model explains the agonist-specific binding properties of the adenylate cyclase-coupled beta-adrenergic receptor. *J Biol Chem* 255:7108–7117.
24. Seifert R, et al. (1998) Different effects of $G_{s\alpha}$ splice variants on β_2-adrenoreceptor-mediated signaling. The β_2-adrenoreceptor coupled to the long splice variant of $G_s\alpha$ has properties of a constitutively active receptor. *J Biol Chem* 273:5109–5116.
25. Hein P, Frank M, Hoffmann C, Lohse MJ, Bunemann M (2005) Dynamics of receptor/G protein coupling in living cells. *EMBO J* 24:4106–4114.
26. Nobles M, Benians A, Tinker A (2005) Heterotrimeric G proteins precouple with G protein-coupled receptors in living cells. *Proc Natl Acad Sci USA* 102:18706–18711.
27. Gales C, et al. (2005) Real-time monitoring of receptor and G-protein interactions in living cells. *Nat Methods* 2:177–184.
28. Peveri P, Heyworth PG, Curnutte JT (1992) Absolute requirement for GTP in activation of human neutrophil NADPH oxidase in a cell-free system: Role of ATP in regenerating GTP. *Proc Natl Acad Sci USA* 89:2494–2498.
29. McKee EE, Bentley AT, Smith RM, Jr, Ciaccio CE (1999) Origin of guanine nucleotides in isolated heart mitochondria. *Biochem Biophys Res Commun* 257:466–472.
30. Kenakin TP (2008) Pharmacological onomastics: What's in a name? *Br J Pharmacol* 153:432–438.
31. Whorton MR, et al. (2007) A monomeric G protein-coupled receptor isolated in a high-density lipoprotein particle efficiently activates its G protein. *Proc Natl Acad Sci USA* 104:7682–7687.
32. Ghanouni P, Steenhuis JJ, Farrens DL, Kobilka BK (2001) Agonist-induced conformational changes in the G-protein-coupling domain of the β_2 adrenergic receptor. *Proc Natl Acad Sci USA* 98:5997–6002.
33. Swaminath G, et al. (2004) Sequential binding of agonists to the β_2 adrenoceptor: Kinetic evidence for intermediate conformational states. *J Biol Chem* 279:686–691.
34. Swaminath G, et al. (2005) Probing the β_2 adrenoceptor binding site with catechol reveals differences in binding and activation by agonists and partial agonists. *J Biol Chem* 280:22165–22171.
35. Yao X, et al. (2006) Coupling ligand structure to specific conformational switches in the β_2-adrenoceptor. *Nat Chem Biol* 2:417–422.
36. Altenbach C, Kusnetzow AK, Ernst OP, Hofmann KP, Hubbell WL (2008) High-resolution distance mapping in rhodopsin reveals the pattern of helix movement due to activation. *Proc Natl Acad Sci USA* 105:7439–7444.
37. Gether U, et al. (1997) Agonists induce conformational changes in transmembrane domains III and VI of the β_2 adrenoceptor. *EMBO J* 16:6737–6747.
38. Jensen AD, et al. (2000) Agonist-induced conformational changes at the cytoplasmic side of transmembrane segment 6 in the β_2 adrenergic receptor mapped by site-selective fluorescent labeling. *J Biol Chem* 276:9279–9290.
39. Ballesteros JA, et al. (2001) Activation of the β_2-adrenergic receptor involves disruption of an ionic lock between the cytoplasmic ends of transmembrane segments 3 and 6. *J Biol Chem* 276:29171–29177.
40. Chidiac P, Hebert TE, Valiquette M, Dennis M, Bouvier M (1994) Inverse agonist activity of beta-adrenergic antagonists. *Mol Pharmacol* 45:490–499.
41. Wisler JW, et al. (2007) A unique mechanism of β-blocker action: Carvedilol stimulates β-arrestin signaling. *Proc Natl Acad Sci USA* 104:16657–16662.
42. Granier S, et al. (2007) Structure and conformational changes in the C-terminal domain of the β_2-adrenoceptor: Insights from fluorescence resonance energy transfer studies. *J Biol Chem* 282:13895–13905.
43. Vilardaga JP, Steinmeyer R, Harms GS, Lohse MJ (2005) Molecular basis of inverse agonism in a G protein-coupled receptor. *Nat Chem Biol* 1:25–28.
44. Ghanouni P, et al. (2001) Functionally different agonists induce distinct conformations in the G protein coupling domain of the β_2 adrenergic receptor. *J Biol Chem* 276:24433–24436.
45. Samama P, Pei G, Costa T, Cotecchia S, Lefkowitz RJ (1994) Negative antagonists promote an inactive conformation of the β_2-adrenergic receptor. *Mol Pharmacol* 45:390–394.
46. Bond RA, et al. (1995) Physiological effects of inverse agonists in transgenic mice with myocardial overexpression of the β_2-adrenoceptor. *Nature* 374:272–276.
47. Azzi M, et al. (2001) Allosteric effects of G protein overexpression on the binding of beta-adrenergic ligands with distinct inverse efficacies. *Mol Pharmacol* 60:999–1007.
48. Kozasa T, Gilman AG (1995) Purification of recombinant G proteins from Sf9 cells by hexahistidine tagging of associated subunits. Characterization of α_{12} and inhibition of adenylyl cyclase by α^z. *J Biol Chem* 270:1734–1741.
49. Ballesteros JA, Weinstein H (1995) Integrated methods for the construction of three-dimensional models and computational probing of structure-function relations in G protein coupled receptors. *Meth Neurosci* 25:366–428.
50. Dundas J, et al. (2006) CASTp: Computed atlas of surface topography of proteins with structural and topographical mapping of functionally annotated residues. *Nucleic Acids Res* 34(Web Server issue):W116–W118.